Efficient scheme for calculating work of adhesion between a liquid and polymer-grafted substrate

Masayuki Uranagase, Shuji Ogata, Kouichi Tanaka, Hodaka Mori, and Satomi Tajima

Citation: The Journal of Chemical Physics **149**, 064703 (2018); doi: 10.1063/1.5028323
View online: https://doi.org/10.1063/1.5028323
View Table of Contents: http://aip.scitation.org/toc/jcp/149/6
Published by the American Institute of Physics

Efficient scheme for calculating work of adhesion between a liquid and polymer-grafted substrate

Masayuki Uranagase,[1,a)] Shuji Ogata,[1,b)] Kouichi Tanaka,[2] Hodaka Mori,[2] and Satomi Tajima[3]
[1]*Department of Physical Science and Engineering, Nagoya Institute of Technology, Nagoya, Aichi 466-8555, Japan*
[2]*DENSO Corporation, 1-1 Showa-cho, Kariya, Aichi 448-8661, Japan*
[3]*Toyota Central R&D Labs., Inc., 41-1 Yokomichi, Nagakute, Aichi 480-1192, Japan*

(Received 9 March 2018; accepted 29 July 2018; published online 13 August 2018)

We propose a method for calculating the work of adhesion between a liquid and solid surface by using molecular simulations. Two ideas are introduced for efficient calculation when the proposed method is applied at the interface between a liquid and a polymer-grafted substrate. First, the liquid molecules are separated from the solid surface based on its shape by placing spherically symmetric potentials around the atoms selected from the substrate and the polymers grafted onto it. Second, to avoid deterioration of accuracy during numerical integration of the work, the parameters that appear in the potential are updated so that variations in the gradient of the work are suppressed. This method is applied to the interface between water and a gold substrate modified by poly(ethylene oxide) (PEO), and it is found that the work of adhesion is greater at intermediate PEO densities. *Published by AIP Publishing.* https://doi.org/10.1063/1.5028323

I. INTRODUCTION

Understanding the properties of a liquid on a solid surface is important from the viewpoint of industrial applications such as wetting, adhesion, and lubrication.[1] Solid-liquid interfacial free energy γ_{SL} is one of the key quantities that characterize the physical properties of the interface. The solid-liquid interfacial free energy is related to the contact angle θ between a liquid droplet and a solid surface via Young's equation[1]

$$\gamma_{SL} = \gamma_S - \gamma_L \cos\theta, \tag{1}$$

where $\gamma_{S(L)}$ is the surface free energy of the solid(liquid). This equation implies that a liquid is wettable on the solid surface, that is, θ becomes small, when γ_{SL} is small. Moreover, the solid-liquid interfacial free energy is closely related to the property of adhesion. Adhesion strength is quantitatively evaluated in terms of the work of adhesion W, a type of free energy, which is defined as the work necessary for separating two contiguous materials.[2,3] The work of adhesion is expressed using γ_S, γ_L, and γ_{SL} as

$$W = \gamma_S + \gamma_L - \gamma_{SL}. \tag{2}$$

Strong adhesion is related to small γ_{SL}. The importance of the solid-liquid interfacial free energy is not limited to the problem of wetting and adhesion. For example, in classical nucleation theory, the free energy barrier of nucleation, such as crystal growth, can be evaluated from the solid-liquid interfacial free energy.[4]

Because the solid-liquid interfacial free energy is essential for elucidating the physical properties of solid-liquid interfaces, it is important to establish a method for accurate evaluation of the solid-liquid interfacial free energy. In principle, the solid-liquid interfacial free energy can be evaluated by laboratory experiments, for example, through the contact angle. However, such a contact angle often contains a non-negligible error. Therefore, molecular simulations, which offer sophisticated methods for calculating the free energy,[5] are expected to be used for accurate evaluation of the solid-liquid interfacial free energy. Several molecular simulation methods based on thermodynamic integration have been proposed to evaluate the solid-liquid interfacial free energy.[6–15] The main operation in these methods is separation or contact of a liquid and a solid surface by introducing an artificial potential. For example, the phantom wall method[9–11] uses planar external potential to separate liquid molecules from a solid surface. The solid-liquid interfacial free energy can be calculated by integrating the force exerted on this potential by liquid molecules.

Recently, experimental techniques that change the physical and chemical properties of solid surfaces have attracted considerable attention, for example, plasma-surface modification,[16] polymer brush,[17] and self-assembled monolayer.[18] Because of this treatment, the surface structure often becomes complex. Thus far, a proper method for calculating the solid-liquid interfacial free energy of such a complex solid surface has not been established. This is because the existing methods can be applied only to smooth and flat solid surfaces.

In this paper, we propose a novel free energy calculation method that can be applied to interfaces involving polymer-grafted surfaces. Additional potentials with spherical symmetry are placed around the atoms selected from the complex solid surface according to its structure to separate liquid molecules

a) uranagase.masayuki@nitech.ac.jp
b) ogata@nitech.ac.jp

from the solid surface. This method is then applied to the interface between water and a gold substrate modified by poly(ethylene oxide) (PEO). Notably, the proposed method directly calculates the work of adhesion as opposed to the interfacial free energy. The work of adhesion and the interfacial free energy are related to each other through the contact angle. From Eqs. (1) and (2), the work of adhesion can be expressed as

$$W = \gamma_{\mathrm{L}}(1 + \cos\theta). \tag{3}$$

That is, not only adhesive properties but also wetting properties are evaluated quantitatively by the work of adhesion.

The remainder of this paper is organized as follows. Section II describes the methods used to calculate the work of adhesion. In Sec. III, the proposed method is used to investigate the dependence of work of adhesion between water and the gold substrate modified by PEO on the density of PEO. Then, the parameter update scheme that appears in the potential to suppress sharp changes in the free energy gradient is discussed; this scheme is required for enhancing accuracy during numerical integration. Section IV presents our concluding remarks.

II. SCHEME FOR CALCULATION OF WORK OF ADHESION

We assume that the system is dependent on the parameter λ. λ-dependent free energy $F(\lambda)$ of the system can be formulated using the integral of its derivative as follows:

$$F(\lambda) = \int_{\lambda_0}^{\lambda} \frac{\partial F}{\partial \lambda'} d\lambda' + F(\lambda_0), \tag{4}$$

where λ_0 is the value of λ in the reference state. When the system depends on λ only via the Hamiltonian H, the integrand in Eq. (4) is given by

$$\frac{\partial F}{\partial \lambda'} = \left\langle \frac{\partial H}{\partial \lambda'} \right\rangle, \tag{5}$$

where $\langle A \rangle$ denotes the ensemble average of A.

To calculate the work of adhesion, an additional potential V_{add} that depends on λ is introduced to separate the liquid molecules from the solid surface by gradually changing λ. In this method, the Hamiltonian of the system is written as follows:

$$H(\boldsymbol{p}, \boldsymbol{q}, \lambda) = H_0(\boldsymbol{p}, \boldsymbol{q}) + V_{\mathrm{add}}(\boldsymbol{p}, \boldsymbol{q}, \lambda), \tag{6}$$

where $\boldsymbol{p}$ and $\boldsymbol{q}$ are the momentum and coordinate of particles in the system, respectively, and $H_0(\boldsymbol{p}, \boldsymbol{q})$ is the Hamiltonian of the original system. From Eqs. (5) and (6), the integrand in Eq. (4) is expressed as

$$\frac{\partial F}{\partial \lambda'} = \left\langle \frac{\partial V_{\mathrm{add}}}{\partial \lambda'} \right\rangle. \tag{7}$$

Molecular dynamics simulations facilitate the evaluation of Eq. (7) by replacing the ensemble average with the time average because V_{add} must be defined explicitly in advance.

In previous studies related to calculation of the solid-liquid interfacial free energy by using molecular simulations,[9,11,12,14,15] V_{add} was taken as the external potential of planar shape. Accordingly, λ is related to the distance from the solid surface and a change in λ corresponds to a shift in the position of the potential along the direction normal to the solid surface. However, the previous methods are inefficient when applied to a solid surface modified by polymers. For example, if the liquid molecules reach near the surface of the substrate, it is necessary to shift the external potential over long distances to completely separate the liquid molecules from the solid surface. This situation is encountered when the density of the polymer grafted onto the solid surface is low. To avoid this inefficiency, we introduce potentials with spherical symmetry that are placed around atoms in both the polymers and the substrate. This facilitates separation of the liquid molecules from the solid surface according to its shape.

To construct the spherical potential, the following conditions are imposed. First, the potential should be smooth as a function of the distance r from the center of the spherical potential. Here, we assume that the potential is continuous until the second-order derivative. Second, it is desirable that the potential is finite at all values of r because the potential must converge uniformly to zero at the limit where the potential vanishes for all values of r. Third, the potential has both repulsive and attractive parts. Although a liquid molecule is separated using the repulsive part of the potential, the shape of the liquid surface changes spontaneously after sufficient separation, if there is no attractive part in the potential. This spontaneous change must be avoided because the change in the free energy related to this change cannot be evaluated. Considering these conditions, we can define the form of the spherical potential V_{sph} as follows:

$$V_{\mathrm{sph}}(r;\lambda) = \begin{cases} [C_1 + C_2 \exp(-C_3 r)]^{-1} + C_4, & 0 \leqslant r \leqslant R_0\sigma(\lambda), \\ V_{\mathrm{LJ}}(r;\lambda) - V_{\mathrm{LJ}}(R_{\mathrm{c}}\sigma(\lambda);\lambda) - V'_{\mathrm{LJ}}(R_{\mathrm{c}}\sigma(\lambda);\lambda)(r - R_{\mathrm{c}}\sigma(\lambda)), & \\ -0.5V''_{\mathrm{LJ}}(R_{\mathrm{c}}\sigma(\lambda);\lambda)(r - R_{\mathrm{c}}\sigma(\lambda))^2, & R_0\sigma(\lambda) < r \leqslant R_{\mathrm{c}}\sigma(\lambda), \end{cases} \tag{8}$$

where $V_{\mathrm{LJ}}(r;\lambda)$, $V'_{\mathrm{LJ}}(R_{\mathrm{c}}\sigma(\lambda);\lambda)$, and $V''_{\mathrm{LJ}}(R_{\mathrm{c}}\sigma(\lambda);\lambda)$ are defined as follows:

$$V_{\mathrm{LJ}}(r;\lambda) \equiv V_{\mathrm{LJ}}(r;\varepsilon(\lambda),\sigma(\lambda)) = 4\varepsilon(\lambda)\left\{\left(\frac{\sigma(\lambda)}{r}\right)^{12} - \left(\frac{\sigma(\lambda)}{r}\right)^{6}\right\},$$

$$V'_{\mathrm{LJ}}(R_{\mathrm{c}}\sigma(\lambda);\lambda) = \left.\frac{\partial V_{\mathrm{LJ}}(r;\lambda)}{\partial r}\right|_{r=R_{\mathrm{c}}\sigma(\lambda)},$$

$$V''_{\mathrm{LJ}}(R_{\mathrm{c}}\sigma(\lambda);\lambda) = \left.\frac{\partial^2 V_{\mathrm{LJ}}(r;\lambda)}{\partial r^2}\right|_{r=R_{\mathrm{c}}\sigma(\lambda)}.$$

Equation (8) includes parameters $C_i (i = 1, \ldots, 4)$, R_0, and R_c. The C_i's are determined from the continuity condition at $r = R_0\sigma(\lambda)$ up to the second derivative and from the value of $V_{sph}(r; \lambda)$ at $r = 0$. $V_{sph}(0; \lambda)$ should be determined such that this potential surely separates the liquid molecules from the solid surface. Here, we set $V_{sph}(0; \lambda) = 20\varepsilon(\lambda)$ because we confirmed that the potential successfully separates the liquid molecules. A small R_c is desirable from the viewpoint of computational cost. However, if R_c is too small, the potential cannot retain the structure of the liquid surface and it changes spontaneously. To avoid this, we set R_c to 1.6. It is necessary to choose R_0 such that $V_{LJ}(R_0\sigma(\lambda); \lambda)$ is less than $V_{sph}(0; \lambda)$, although the results are not sensitive to R_0. Here, R_0 is set to 1.01.

Using the potentials defined above, the liquid molecules are separated from the solid surface by executing the following operations, which are schematized in Fig. 1.

(P1) Atoms are selected from the substrate, and the polymers grafted onto the substrate. The centers of spherically symmetric potentials are set to the positions of these atoms.

(P2) Liquid molecules are separated gradually from the solid surface by increasing σ in the potential. The difference in free energy between the final and the initial states in this operation is denoted by ΔF_2.

(P3) When the liquid is separated sufficiently from the solid surface, the solid surface rarely affects the liquid molecules. Then, the interaction potentials between the atoms of the liquid and of the solid are set to 0. This operation is considered as decoupling of the solid surface from the liquid. The free energy change ΔF_3 due to this operation is expected to be extremely small compared to (P2) and (P4) owing to relatively weak interactions between the liquid and the solid surface. Therefore, we can safely suppose that $\Delta F_3 = 0$.

(P4) The diameter of the potential is decreased gradually; finally, the system recovers the state without an additional potential, but the liquid is decoupled from the solid surface. Differences in the free energy between the final and the initial states in this operation are denoted by ΔF_4.

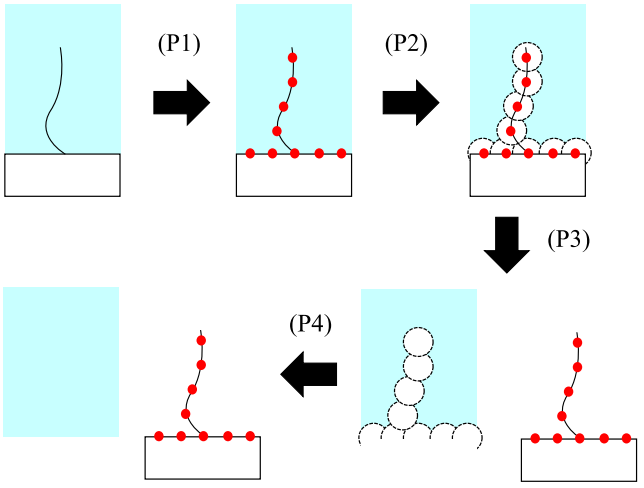

FIG. 1. Schematic diagram of calculation of work of adhesion. (P1) Selection of the centers of potentials from the atoms consisting of a complex solid surface. (P2) Separation of the liquid molecules from the solid surface. (P3) Decoupling of the solid surface from the liquid. (P4) Recovery of the system with no added potential.

Because the final state in (P4) is simply the state in which the liquid and the solid surface exist independently, the work of adhesion is equivalent to the free energy difference between the final state in (P4) and the initial state in (P2). Thus, the work of adhesion is obtained as the summation of the free energy changes in each operation, that is, $\Delta F_2 + \Delta F_4$.

III. APPLICATION TO WATER-GOLD SUBSTRATE MODIFIED BY PEO INTERFACE

The proposed method is applied to the interface between the water and the gold substrate modified by PEO by using our original molecular dynamics simulation code. The gold substrate modified by PEO has attracted considerable attention because it resists protein adsorption despite the fact that proteins are generally adsorbed on most surfaces.[19] Detailed experiments on the behaviors of protein when placed on polymer-grafted surfaces have revealed that several conditions must be fulfilled for the surface to resist protein adsorption. Hydrophilicity of the surface is one such condition.[20] Thus, it is worthwhile to investigate the hydrophilicity of the surface of the gold substrate surface. Several studies have evaluated the behavior of water on a gold substrate modified by PEO via molecular simulations.[21–23]

The interface between water and the gold substrate modified by PEO treated in the present work is modeled as follows. The size of the gold substrate is 6.90, 2.99, and 1.40 nm, in the $[\bar{1}10]$, $[\bar{1}\bar{1}2]$, and [111] directions, respectively, and the (111) surface is modified by PEO, the formula of which is $CH_3(OCH_2CH_2)_6CH_2SH$. Note that PEO is grafted onto the gold surface so that the SH group becomes a head group and grafting points comprise a $(\sqrt{3} \times \sqrt{3})R30°$ lattice when PEO is fully grafted onto the gold surface. This configuration is observed in the self-assembled monolayer of alkanethiol molecules on a gold substrate by using scanning tunneling microscopy.[24–26] In reality, the self-assembled monolayer may be composed of polymers of varying lengths. To mimic such a mixed self-assembled monolayer, PEO is replaced by the shorter alkyl molecule CH_3CH_2SH when the coordinate of the grafting point in the $[\bar{1}10]$ direction exceeds the threshold value defined in advance. Hence, the surface of the gold substrate is clearly separated into two parts: one is modified by PEOs and the other by shorter alkyl molecules. We define a normalized density ρ as $N_{PEO}/(N_{PEO} + N_{Alkyl})$, where N_{PEO} and N_{Alkyl} denote the number of PEO and alkyl molecules, respectively. 3000 water molecules are placed on the top surface of the gold substrate modified by PEOs. Periodic boundary conditions are applied along three directions. The dimensions of the simulation cell are 6.90, 2.99, and 12.0 nm in the $[\bar{1}10]$, $[\bar{1}\bar{1}2]$, and [111] directions of the gold substrate, respectively. The dimensions of the simulation cell in the [111] direction are selected such that the vacuum space between the top surface of the water and the bottom of the gold substrate is longer than 3 nm.

Gold atoms interact according to the Lennard-Jones potential, whose parameters are determined such that the surface tension is equivalent to the experimental value, instead of cohesive energy.[27] Interactions among PEO molecules and those between PEO molecules and water molecules are treated using the force field parameterized in Ref. 28. The TIP4P model[29] is adopted for the water molecules because the force field parameterization in Ref. 28 assumes the use of this model. Interactions between the grafting polymer and the gold atoms are evaluated using the force field in Ref. 30. Notably, the sulfur atom in the PEO bonds to the gold atom on the surface, and the hydrogen atom that is originally bonded to the sulfur atom dissociates. The cutoff length of the Lennard-Jones potential is set to thrice the value of the parameter corresponding to the diameter appeared in the potential. A few of the interactions between atoms are expressed by the Buckingham potential instead of the Lennard-Jones potential. The cutoff length of the Buckingham potential is determined such that the ratio of the potential at the cutoff length to the value of the local minimum is equal to the value of the Lennard-Jones potential.

Equations of motion are integrated numerically by using the velocity Verlet method. We must solve equations of motion for rotational degrees of freedom in the water molecules because the TIP4P model represents the water molecule as a rigid body. For efficient computation of the rotational degrees of freedom, the algorithm proposed by Kajima *et al.*[31] is used. This algorithm was successfully applied to a system consisting of rigid water molecules.[32] We set the time step for integration to 2 fs. In general, this time step is relatively large for systems containing hydrogen atoms. Here, the mass of the hydrogen atom was set to be identical to that of the carbon atom to avoid rapid hydrogen movement, which decreases the accuracy of the solutions of the aforementioned equations of motion. Note that this change should not affect calculation of the work of adhesion because this quantity is determined only from the configurational part of the partition function. System temperature T is maintained at 300 K by applying the velocity rescaling method developed by Bussi *et al.*[33] Coulomb interactions were evaluated using the standard Ewald method. In this method, an adjustable parameter, α, is used to split $1/r$ into two terms, namely, $\mathrm{erf}(\alpha r)/r$ and $\mathrm{erfc}(\alpha r)/r$. Here, α was set to 2.1 nm^{-1}. The cutoff length in real space and the cutoff magnitude of the wave number in reciprocal space were set to 1.49 nm and 13.85 nm^{-1}, respectively.

In Fig. 2(a), $\partial F/\partial\lambda$ is shown for the case of $\rho = 0.25$. As shown in Fig. 2(b), we set $\varepsilon = 12.5$ kJ/mol and $\sigma = 0.9\lambda$ nm. Sulfur, carbon, and oxygen atoms in polymers and the surface gold atoms were selected as the centers of the spherical potentials that act on the center of mass of each water molecule. Each data point was evaluated for 1 ns in the simulation. When λ increased from 0, $\partial F/\partial\lambda$ had a negative value, corresponding to the attraction of the water molecules near the atoms selected as the centers of potential. When λ exceeded 0.28, $\partial F/\partial\lambda$ increased with λ. This increase was ascribed to potential repulsion that forced away the water molecules around the polymers or the substrate. Upon increasing λ further, we observed a decrease in $\partial F/\partial\lambda$. This property can be attributed to a decrease in force that is necessary for the potentials to push out the water molecules owing to separation from the solid surface. In addition, spread of the attractive part of the potentials contributes toward this decrease. It seems unusual that $\partial F/\partial\lambda$ decreases at such a large value of λ because this results in a decrease in the free energy calculated by numerical integration. Notably, this decrease in the free energy should be compensated for by the free energy calculated in (P4). Thus, the behavior of $\partial F/\partial\lambda$ can be explained by the interactions between the water molecules and the spherical potentials. However, sharp variation in $\partial F/\partial\lambda$, as shown in Fig. 2(a), is unfavorable from the viewpoint of numerical accuracy. Generally, the numerical integration of a function with sharp variations requires function values at shorter intervals to prevent any decrease in accuracy. If $\partial F/\partial\lambda$ varies sharply, the value of $\partial F/\partial\lambda$ should be evaluated at shorter intervals of λ. This can be avoided by finding an appropriate scheme for updating the parameters in the potential that suppresses sharp variations in $\partial F/\partial\lambda$.

Below, both σ and ε are changed along with λ to examine that the ways in which sharp variations in $\partial F/\partial\lambda$ can be suppressed. Then, $\partial F/\partial\lambda$ is evaluated as follows:

$$\frac{\partial F}{\partial\lambda} = \left\langle \frac{\partial\sigma}{\partial\lambda}\frac{\partial V_{\mathrm{sph,all}}}{\partial\sigma} \right\rangle + \left\langle \frac{\partial\varepsilon}{\partial\lambda}\frac{\partial V_{\mathrm{sph,all}}}{\partial\varepsilon} \right\rangle, \tag{9}$$

where $V_{\mathrm{sph,all}}$ represents all potentials added to the system. Changes in σ are identical to the above case, that is, $\sigma = 0.9\lambda$ nm. In Fig. 3(a), we show $\partial F/\partial\lambda$ as a function of λ, where σ and ε change, as shown in Fig. 3(b). Both increases and decreases in $\partial F/\partial\lambda$ are suppressed as the changes in ε become large. The exact expression of ε is given in Eq. (A1) in the Appendix. Small values of ε at small λ suppress the

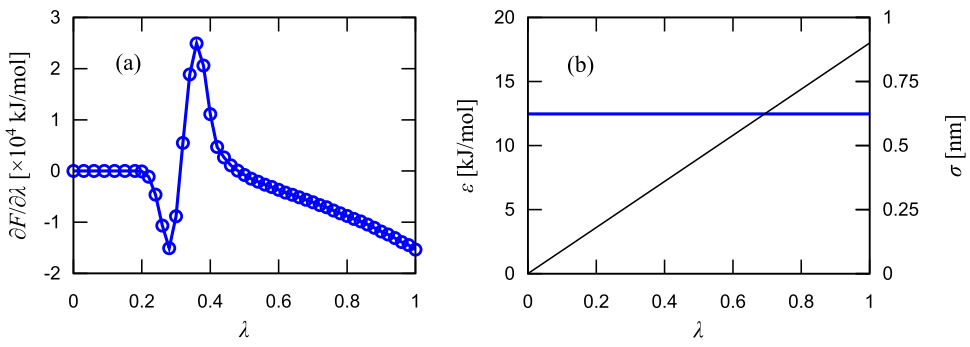

FIG. 2. (a) $\partial F/\partial\lambda$ for $\rho = 0.25$ in (P2). (b) ε (thick blue line) and σ (thin black line) as functions of λ.

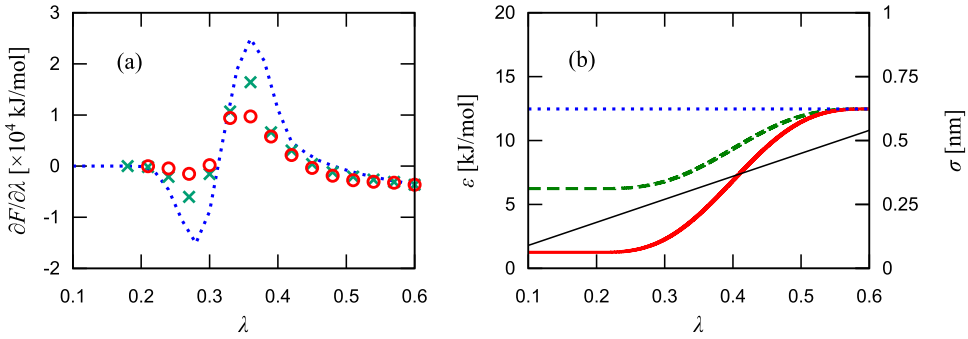

FIG. 3. (a) $\partial F/\partial\lambda$ for $\rho = 0.25$ in (P2) at small λ. Red circles, green crosses, and blue dotted curves are obtained by setting ε_1 in Eq. (A1) to 1.25, 6.25, and 12.5 kJ/mol, respectively. (b) λ dependence of ε. Thick red solid, green dashed, and blue dotted curves are obtained by setting ε_1 in Eq. (A1) to 1.25, 6.25, and 12.5 kJ/mol, respectively. λ_1, λ_2, and ε_2 in Eq. (A1) are 0.2, 0.6, and 12.5 kJ/mol, respectively, in all cases. The λ dependence of σ is plotted as a thin black line.

initial decrease in $\partial F/\partial\lambda$. As mentioned above, the increase in $\partial F/\partial\lambda$ can be ascribed to the force to push out the water molecules, which corresponds to the first term on the right-hand side of Eq. (9). Increases in $\partial F/\partial\lambda$ must be restrained because such increases are partially cancelled by the decrease in the potential energy due to increase in ε, which corresponds to the second term on the right-hand side of Eq. (9). Note that the value of $\partial F/\partial\lambda$ at $\lambda = 0.6$ is nearly identical for every case. This is plausible because a state with the same variables does not depend on the intermediate state.

We can further suppress variations in $\partial F/\partial\lambda$ by carefully determining the scheme for updating ε. In Fig. 4(a), $\partial F/\partial\lambda$ is shown as a function of λ when ε is varied according to the thick red curve in Fig. 4(b). Here, we did not use Eq. (A1) for updating ε because there are limitations in updating ε by using Eq. (A1), which are attributed to the symmetricity of the equation, as mentioned in the Appendix. Instead, we used Eq. (A2) from the Appendix to obtain the thick red curve in Fig. 4(b). In Fig. 4(c), a few snapshots corresponding to Fig. 4(a) are displayed. The snapshot of the final state clearly shows that the water molecules are separated according to the solid surface structure.

In Fig. 5, we show $\partial F/\partial\lambda$ for cases $\rho = 0, 0.5, 0.75$, and 1.0 during (P2). The dependences of ε and σ on λ are identical to that shown in Fig. 4(b). Changes in $\partial F/\partial\lambda$ become relatively small for all cases. This suggests that the scheme for updating σ and ε defined for one specific case of suppressing variations in $\partial F/\partial\lambda$ can be applied to other densities to obtain a similar effect.

We arrived at the aforementioned update scheme heuristically. Here, we considered the physical meaning of this scheme, which will be helpful for generalizing this method. The condition that $\partial F/\partial\lambda$ approaches 0 can be written from Eq. (9) as

$$\frac{\partial\sigma}{\partial\lambda}\left\langle\frac{\partial V_{\mathrm{sph,all}}}{\partial\sigma}\right\rangle + \frac{\partial\varepsilon}{\partial\lambda}\left\langle\frac{\partial V_{\mathrm{sph,all}}}{\partial\varepsilon}\right\rangle = 0. \tag{10}$$

We considered the dependence of ε on λ which satisfies Eq. (10). To obtain $\partial\varepsilon/\partial\lambda$, the ensemble averages of

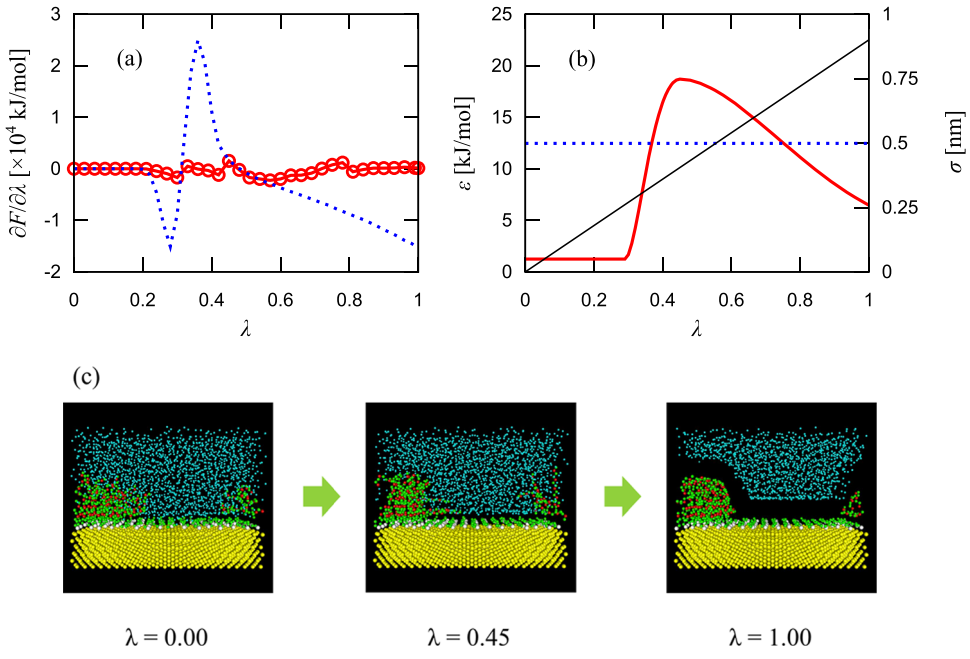

FIG. 4. (a) $\partial F/\partial\lambda$ for $\rho = 0.25$ in (P2) for an appropriately determined ε (red circles). The blue dotted curve is the same result as that in Fig. 2(a). (b) Thick red curve and the blue dotted curve are ε as a function of λ used to obtain the red circles and blue dotted curve in (a), respectively. The thick red curve is plotted according to Eq. (A2) with the parameters shown in the Appendix. The λ dependence of σ is plotted as a thin black line. (c) Snapshots at $\lambda = 0$, 0.45, and 1. The green, red, white, yellow, and light blue spheres represent carbon, oxygen in PEO, sulfur, gold, and oxygen in the water molecules, respectively. The hydrogen atoms in polymers and the water molecules are omitted.

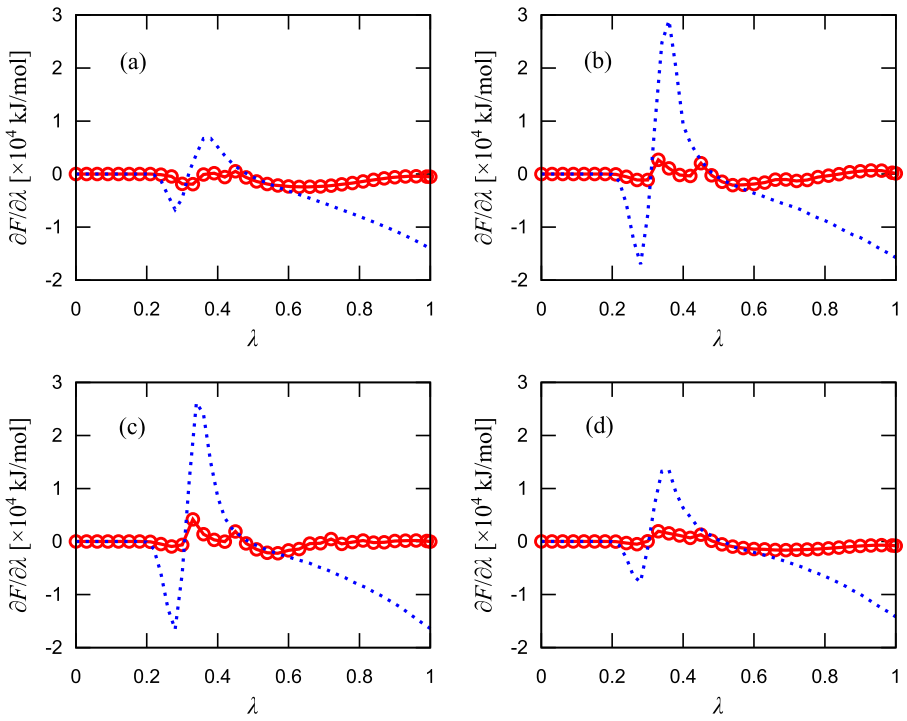

FIG. 5. $\partial F/\partial\lambda$ for ρ = 0 (a), 0.5 (b), 0.75 (c), and 1.0 (d) in (P2) for constant (blue dotted curve) and an appropriately determined (red circles) ε. Update scheme of σ and ε is the same as that in Fig. 4(b).

$\partial V_{\mathrm{sph,all}}/\partial\sigma$ and $\partial V_{\mathrm{sph,all}}/\partial\varepsilon$ should be evaluated. Here, we roughly approximated the ensemble average of A by

$$\langle A\rangle = \int_0^{R_c\sigma} A(r)\rho_w(r)4\pi r^2 dr, \tag{11}$$

where r and $\rho_w(r)$ represent the distance from the center of the potential and the density profile of the water molecule, respectively. Figure 6(a) shows the dependence of ε on λ, which was determined such that Eq. (10) was satisfied. We assume that ρ_w is proportional to $\exp(-V_{\mathrm{sph}}(r)/k_BT)$, where k_B is Boltzmann's constant. The initial condition was set to ε = 2.89 kJ/mol at λ = 0.3. This value of ε is larger than that used in Fig. 4(b) because ε gradually approaches 0 as λ increases if the initial value is set similar to that used in Fig. 4(b). There is a threshold value for the initial condition of ε at which the behavior of the solution to Eq. (10) changes qualitatively. We found that this threshold value is 2.70 kJ/mol. Notably, the value of ε is almost identical to that used in Fig. 4(b) despite it being approximated roughly. The reason for the deviation at small values of λ, except for the difference in the initial

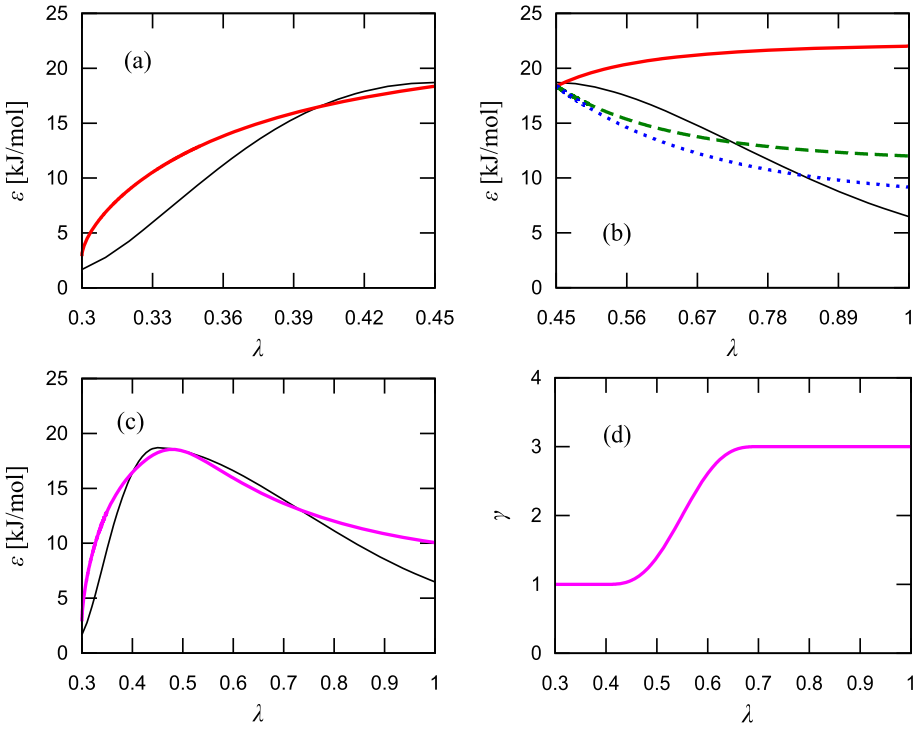

FIG. 6. (a) λ dependence of ε determined to satisfy Eq. (10) at a small λ (thick red curve). The thin black curve is the same as the thick red curve in Fig. 4(b). (b) λ dependence of ε to satisfy Eq. (10) at large λ with γ = 1 (thick red solid curve), 2 (green dashed curve), and 3 (blue dotted curve). The thin black curve is the same as the thick red curve in Fig. 4(b). (c) Solution of Eq. (10) when γ changes smoothly (thick purple curve). The thin black curve is the same as the thick red curve shown in Fig. 4(b). (d) Update of γ to obtain the result in (c).

value, is because Eq. (A2) imposes the condition $\partial\varepsilon/\partial\lambda = 0$ at both endpoints. This condition results in a slow increase in ε at small λ.

When the value of λ becomes large, a water molecule near the solid surface is exposed to forces resulting from more than one potential. In this case, if we continue to calculate ε for large values of λ that satisfy Eq. (10), ε increases with λ, as shown by the thick red solid curve in Fig. 6(b). This pattern is different from that used in our simulations. One of the methods to modify this pattern involves assuming ρ_w proportional to $\exp(-\gamma V_{sph}(r)/k_B T)$, where γ is an adjustable parameter. In Fig. 6(b), the dependence of ε on λ for $\gamma = 2$ and 3 is shown, where ε decreases as λ increases. Here, γ may be regarded as the factor corresponding to the change in energy because of the effects of more than one potential.

The above results suggest that the behavior of ε, which is similar to that shown in Fig. 4(b) can be replicated by smoothly changing γ with λ. Figure 6(c) shows the solution of Eq. (10) when γ changes according to Fig. 6(d). The equation used to update γ exhibits the same form as Eq. (A1), in which ε is replaced by γ. Note that the update scheme for ε, which was obtained heuristically can be reproduced fairly well despite rough approximation of the interactions between the water molecules and the potentials. The results in Fig. 4(b) can be reproduced with high accuracy by appropriately taking realistic conditions into account, for example, the dependence of γ on r.

Thus far, we have discussed the behavior of $\partial F/\partial\lambda$ during (P2). To obtain the work of adhesion, the free energy difference in (P4) should be evaluated. In Fig. 7, we plot $\partial F/\partial\lambda$ for the cases of $\rho = 0$, 0.25, 0.5, 0.75, and 1.0 in (P4). Here, both σ and ε change linearly with λ, as shown in Fig. 7(f). Unlike the case of (P2), the behavior of $\partial F/\partial\lambda$ is sufficiently monotonic for all cases. This behavior is suitable from the viewpoint of numerical integration. Hence, we do not pursue further optimal parameter update schemes for the potential in (P4).

The free energy difference was obtained by numerically integrating the $\partial F/\partial\lambda$ shown in Figs. 4, 5, and 7. In Fig. 8(a), ΔF_2 and ΔF_4 are plotted, where numerical integration was performed according to the trapezoidal rule. Figure 8(b) shows the work of adhesion W, which was calculated as the sum of ΔF_2 and ΔF_4. Note that the planar surface area of the substrate was used to evaluate the work of adhesion per unit area, although the curved surface of water appeared in the process of the separation, as shown in Fig. 4(c). W decreased small at $\rho = 0$ and 1, and it was nearly identical for $\rho = 0.25$, 0.5, and 0.75. When $\rho = 0$, no hydrophilic part was observed in the polymers grafted onto the substrate. By contrast, when $\rho = 1$, the water

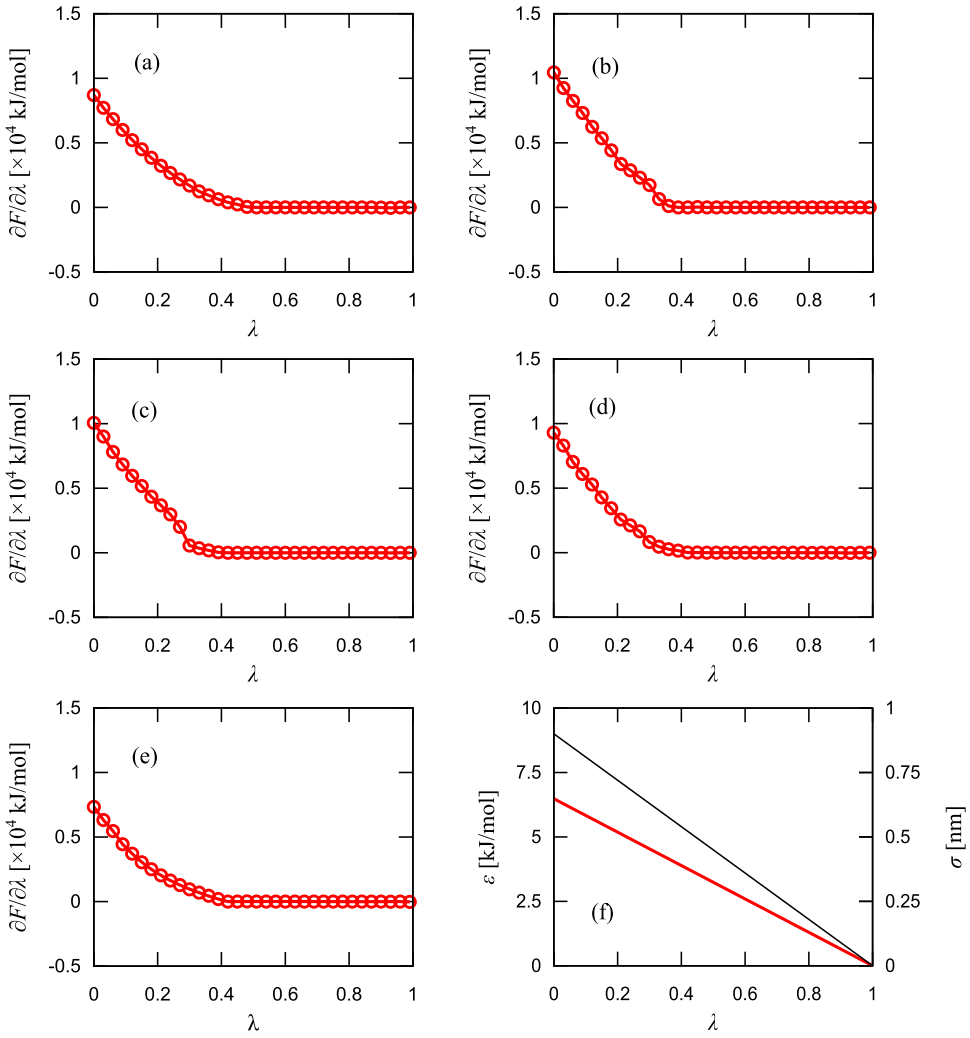

FIG. 7. $\partial F/\partial\lambda$ for $\rho = 0$ (a), 0.25 (b), 0.5 (c), 0.75 (d), and 1.0 (e) in (P4). ϵ (thick red line) and σ (thin black line) change linearly with λ (f).

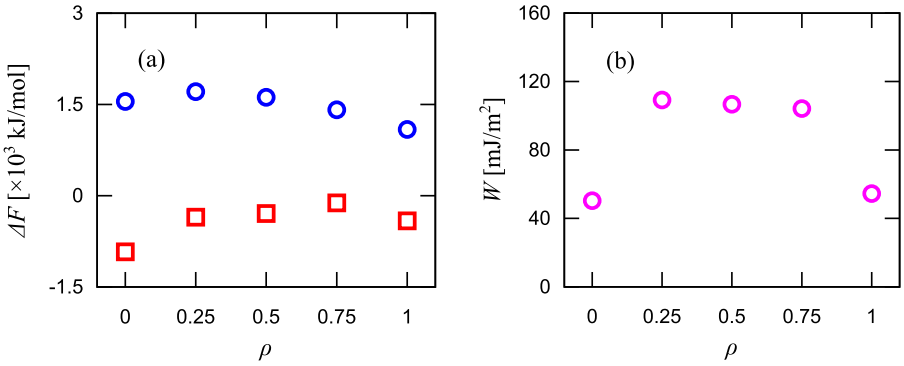

FIG. 8. (a) Free energy difference ΔF_2 (square) and ΔF_4 (circle). (b) Work of adhesion obtained from (a).

molecules could not access the hydrophilic region in the PEO because of the excluded volumes of PEO that were densely grafted onto the substrate. Hence, the work of adhesion was small for $\rho = 0$ and 1.

In the model adopted herein, the region modified by PEOs is clearly separated from that modified by shorter alkyl molecules, and the boundary between them is parallel to $[\bar{1}\bar{1}2]$. For this surface, the number of water molecules that have access to oxygen atoms in PEO remains almost the same even if ρ is changed. This results in an almost constant value of W for cases with intermediate values of ρ. The situation is different in the case in which polymers are grafted randomly onto the surface,[34] although the interface model used in Ref. 34 is different from that used in the present study. This suggests that the work of adhesion depends on the microscopic structures on the surface even though the density of the grafted PEO remains the same.

IV. CONCLUSION

A method to calculate the work of adhesion appropriate for the interface between a liquid and a polymer-grafted solid surface was developed herein by using two novel ideas. First, spherically symmetric potentials were introduced to separate the liquid molecules from the solid surface according to its shape. Second, a parameter update scheme for the potentials was defined so that sharp variations in the free energy gradient are suppressed when the liquid molecules are separated gradually from the solid surface. The proposed method was applied at the interface between water and a gold substrate modified by PEO. We found that the work of adhesion is the maximum at intermediate densities of grafted PEO. This is because the water molecules have access to oxygen atoms in PEO at intermediate densities; however, there are few water molecules near the oxygen atoms in PEO when PEO is fully grafted onto the gold surface.

ACKNOWLEDGMENTS

This study was partially supported by the Ministry of Education, Culture, Sports, Science, and Technology (MEXT) of Japan as a social and scientific priority issue (creation of new functional devices and high-performance materials to support next-generation industries; CDMSI) to be tackled by using post-K computer. Simulations were performed on Fujitsu PRIMEHPC FX100 provided by the Information Technology Center of Nagoya University through the HPCI System Research project (Project ID Nos. hp160028 and hp170037). Computational resources of the K computer provided by the RIKEN Advanced Institute for Computational Science, Fujitsu PRIMERGY at Research Center for Computational Science (Okazaki), and SGI ICE XA/UV and Fujitsu PRIMEHPC FX10 at the Supercomputer Center, the Institute for Solid State Physics, the University of Tokyo were also used in this study.

APPENDIX: UPDATE SCHEME OF ε TO REDUCE CHANGES IN FREE ENERGY GRADIENT

In this appendix, we consider the update scheme for ε at the potential between λ_1 and λ_2. The values of ε at $\lambda = \lambda_1$ and λ_2 are ε_1 and ε_2, respectively. Several nonlinear update schemes are available for ε. The schemes adopted in this paper are introduced herein. First, the triangular function is used as follows:

$$\varepsilon(\lambda;\lambda_1,\lambda_2,\varepsilon_1,\varepsilon_2) = \varepsilon_1 + (\varepsilon_2-\varepsilon_1)\left[f(\lambda;\lambda_1,\lambda_2) - \frac{\sin\{2\pi f(\lambda;\lambda_1,\lambda_2)\}}{2\pi}\right], \tag{A1}$$

where $f(\lambda;\lambda_1,\lambda_2) \equiv (\lambda-\lambda_1)/(\lambda_2-\lambda_1)$. In this scheme, a symmetry around $\bar{\lambda} = (\lambda_1+\lambda_2)/2$ is observed such that $\varepsilon(\bar{\lambda}) = (\varepsilon(\bar{\lambda}+\lambda)+\varepsilon(\bar{\lambda}-\lambda))/2$ for any λ. This symmetry restricts the flexibility for updating ε. Instead of Eq. (A1), the following equation is used:

$$\varepsilon(\lambda;\lambda_1,\lambda_2,\varepsilon_1,\varepsilon_2,\beta) = c_1 + c_2\lambda^\beta\left[\frac{1}{3}\lambda^{2\beta} - \frac{\lambda_1^\beta+\lambda_2^\beta}{2}\lambda^\beta + (\lambda_1\lambda_2)^\beta\right], \tag{A2}$$

where c_1 and c_2 are constants determined to satisfy the condition $\varepsilon = \varepsilon_1$ and ε_2 at $\lambda = \lambda_1$ and λ_2, respectively, and β is a parameter. Figure 4(b) is obtained by setting parameters as follows: $(\lambda_1, \lambda_2, \varepsilon_1, \varepsilon_2, \beta) = (0, 0.29, 1.12, 1.12, 0)$ for $0 \leqslant \lambda < 0.29$, $(0.29, 0.45, 1.12, 18.7, -1)$ for $0.29 \leqslant \lambda \leqslant 0.45$, and $(0.45, 1.2, 18.7, 6.48, 0.5)$ for $0.45 < \lambda \leqslant 1$. These parameters are selected heuristically such that the variation in the free energy gradient is minimized. In Fig. 9, $\partial F/\partial\lambda$ and ε are plotted for the case that one of the parameters is changed from the initial selected value. We confirm that the parameters that we selected (plotted in red circles) successfully suppress variations in $\partial F/\partial\lambda$.

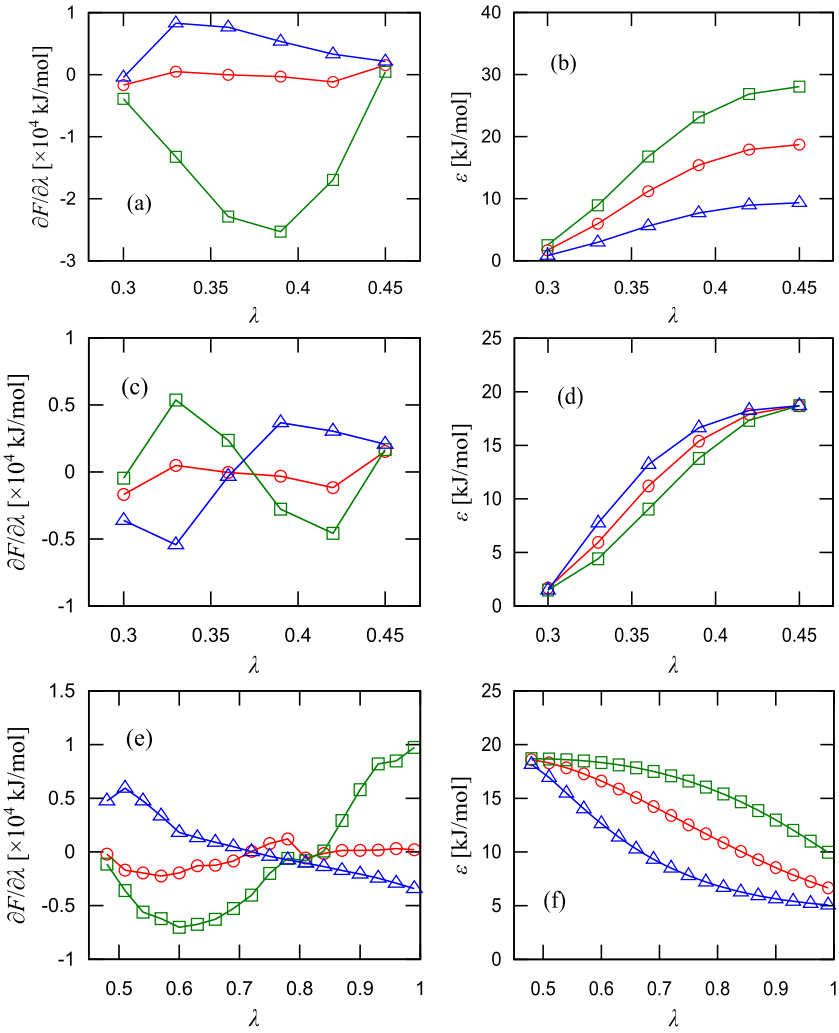

FIG. 9. (a) $\partial F/\partial\lambda$ for $0.29 \leqslant \lambda \leqslant 0.45$. The red circles correspond to the case of $(\lambda_1, \lambda_2, \varepsilon_1, \varepsilon_2, \beta) = (0.29, 0.45, 1.12, 18.7, -1)$. The green squares and the blue triangles are obtained by changing ε_2 to 28.1 and 9.36, respectively, from the case of the red circles. (c) $\partial F/\partial\lambda$ for $0.29 \leqslant \lambda \leqslant 0.45$. The red circles correspond to the case of $(\lambda_1, \lambda_2, \varepsilon_1, \varepsilon_2, \beta) = (0.29, 0.45, 1.12, 18.7, -1)$. The green squares and the blue triangles are obtained by changing β to 0.5 and -2.5, respectively, from the case of the red circles. (e) $\partial F/\partial\lambda$ for $0.45 < \lambda \leqslant 1.0$. The red circles correspond to the case where $(\lambda_1, \lambda_2, \varepsilon_1, \varepsilon_2, \beta) = (0.45, 1.2, 18.7, 6.48, 0.5)$. The green squares and the blue triangles are obtained by changing β to 2.5 and -1.5, respectively, from the case of the red circles. (b), (d), and (f) describe ε when the parameters are set to the same as (a), (c), and (e), respectively.

[1] J. N. Israelachvili, *Intermolecular and Surface Forces*, 3rd ed. (Academic Press, San Diego, 2011).
[2] A. J. Kinloch, J. Mater. Sci. **15**, 2141 (1980).
[3] F. Awaja, M. Gilbert, G. Kelly, B. Fox, and P. J. Pigram, Prog. Polym. Sci. **34**, 948 (2009).
[4] D. W. Oxtoby, J. Phys.: Condens. Matter **4**, 7627 (1992).
[5] *Free Energy Calculations Theory and Applications in Chemistry and Biology*, edited by C. Chipot and A. Pohorille (Springer-Verlag, Berlin, 2007).
[6] J. Q. Broughton and G. H. Gilmer, J. Chem. Phys. **84**, 5759 (1986).
[7] M. Heni and H. Löwen, Phys. Rev. E **60**, 7057 (1999).
[8] R. L. Davidchack and B. B. Laird, Phys. Rev. Lett. **85**, 4751 (2000).
[9] F. Leroy, D. J. V. A. dos Santos, and F. Müller-Plathe, Macromol. Rapid Commun. **30**, 864 (2009).
[10] F. Leroy and F. Müller-Plathe, J. Chem. Phys. **133**, 044110 (2010).
[11] F. Leroy and F. Müller-Plathe, Langmuir **31**, 8335 (2015).
[12] R. Benjamin and J. Horbach, J. Chem. Phys. **137**, 044707 (2012); **139**, 039901 (2013).
[13] R. Benjamin and J. Horbach, J. Chem. Phys. **139**, 084705 (2013).
[14] W. Shou and H. Pan, J. Chem. Phys. **145**, 184702 (2016).
[15] X. Qi, Y. Zhou, and K. A. Fichthorn, J. Chem. Phys. **145**, 194108 (2016).
[16] P. K. Chua, J. Y. Chena, L. P. Wanga, and N. Huangb, Mater. Sci. Eng. R **36**, 143 (2002).
[17] O. Azzaroni, J. Polym. Sci., Part A: Polym. Chem. **50**, 3225 (2012).
[18] J. C. Love, L. A. Estroff, J. K. Kriebel, R. G. Nuzzo, and G. M. Whitesides, Chem. Rev. **105**, 1103 (2005).
[19] K. L. Prime and G. M. Whitesides, Science **252**, 1164 (1991).
[20] Q. Wei, T. Becherer, S. Angioletti-Uberti, J. Dzubiella, C. Wischke, A. T. Neffe, A. Lendlein, M. Ballauff, and R. Haag, Angew. Chem., Int. Ed. **53**, 8004 (2014).
[21] A. J. Perstin and M. Grunze, Langmuir **16**, 8829 (2000).
[22] A. E. Ismail, G. S. Grest, and M. J. Stevens, Langmuir **23**, 8508 (2007).
[23] M. J. Stevens and G. S. Grest, Biointerphases **3**, FC13 (2008).
[24] G. E. Poirier and M. J. Tarlov, Langmuir **10**, 2853 (1994).
[25] G. E. Poirier, Chem. Rev. **97**, 1117 (1997).
[26] F. Schreiber, J. Phys.: Condens. Matter **16**, R881 (2004).
[27] H. Heinz, R. A. Vaia, B. L. Farmer, and R. R. Naik, J. Phys. Chem. C **112**, 17281 (2008).
[28] G. D. Smith, O. Borodin, and D. Bedrov, J. Comput. Chem. **23**, 1480 (2002).
[29] W. L. Jorgensen, J. Chandrasekhar, J. D. Madura, R. W. Impey, and M. L. Klein, J. Chem. Phys. **79**, 926 (1983).
[30] B. Rai, P. Santhish, C. P. Malhotra, Pradip, and K. G. Ayappa, Langmuir **20**, 3138 (2004).
[31] Y. Kajima, M. Hiyama, S. Ogata, R. Kobayashi, and T. Tamura, J. Chem. Phys. **136**, 234105 (2012).
[32] Y. Kajima, S. Ogata, R. Kobayashi, M. Hiyama, and T. Tamura, J. Phys. Soc. Jpn. **83**, 083601 (2014).
[33] G. Bussi, D. Donadio, and M. Parrinello, J. Chem. Phys. **126**, 014101 (2007).
[34] M. Uranagase and S. Ogata, MRS Adv. **3**, 519 (2018).